

THE LUNAR CONCENTRIC CRATER ARCHYTAS G ASSOCIATED WITH AN INTRUSIVE DOME

C. Wöhler¹ and R. Lena² – Geologic Lunar Research (GLR) Group. ¹Daimler Group Research, D-89013 Ulm, Germany; christian.woehler@daimler.com; ²Via Cartesio 144, sc. D, I-00137, Rome, Italy; r.lena@sanita.it

Introduction: Lunar concentric craters represent an anomalous type of impact structures on the Moon [1]. The concentric crater Archytas G in mare Frigoris has first been catalogued as a concentric crater in [2]. According to Fig. 1, it is located on top of a large lunar intrusive dome, termed Ar1 in [3]. The dome Ar1 is the only lunar dome known to date with a concentric crater on its surface. In this contribution we estimate the morphometric properties of Archytas G and of Ar1. Modelling the intrusive dome as the result of flexure-induced uplift by a laccolithic intrusion according to [4] allows to estimate the intrusion depth and the magma pressure occurring during dome formation. Based on our analyses, we discuss possible modes of formation for Archytas G.

Morphometric and spectral analysis, laccolith modelling: We performed a photoclinometric analysis of the concentric crater Archytas G and the associated intrusive dome Ar1, relying on the ground-based and orbital images shown in Figs. 1 and 2. The inferred morphometric properties were used for laccolith modelling according to the framework in [4]. Spectral data were inferred from Clementine UVVIS imagery.

Morphometric properties of Archytas G. The diameter of the outer rim of Archytas G amounts to 6.8 km and that of the inner depression lacking a well-defined rim to 4.0 km. The depth of a fresh lunar impact crater of this size typically amounts to one-fifth of its diameter [5], here corresponding to 1.36 km for the outer rim structure. The observed depth of the concentric crater, however, is much smaller. In the Lunar Orbiter image shown in Fig. 1, the sharp outer rim casts a shadow on the crater interior adjacent to the outer rim. The shadow length indicates an elevation difference of 270 m between the rim crest and the outer part of the crater floor. Relying on a photoclinometric analysis of the Clementine 750 nm image of the concentric crater (Fig. 2), we determined a depth of 100 m for the shallow inner crater and an elevation difference of 80 m between the crest of the outer rim and the surrounding surface. Hence, the overall crater depth amounts to 370 m while the centre of the inner crater lies 290 m below the surrounding surface.

Morphometric properties of Ar1. Large lunar intrusive domes, such as Ga1, M13, and the Valentine dome V1 [6], are characterised by flank slopes always well below 1° and diameters of 30 km and more. The 3D shape of the intrusive dome Ar1 has been determined by photoclinometric analysis of the telescopic low-sun image shown in Fig. 1. We found that Ar1 has a diame-

ter of 33 km and is 70 m high. It may possibly be regarded as being composed of two separate partial domes, an elongated eastern part denoted here by Ar1e with an average diameter of 16 km and a height of 70 m, and a lower western part. The northern part of the surface of Ar1 is crossed by a chain of craters that look like secondaries, while the dome surface is crossed from the southwest to the northeast by a structure resembling a linear rille in the south and a fault in the north. The presence of a fault on the dome Ar1 suggests that its uplift induced vertical rupture of the surface. If we assume that the linear rille is the result of tensional stress, the curvature radius of the dome surface inferred from our 3D analysis yields a thickness of the uppermost mare basalt layer of at least 0.24 km, assuming a typical value of the critical stress of basalt of 13 MPa. The laccolith model in [4] applied according to the numerical scheme suggested in [3] yields an intrusion depth of 3.5 km and a magma pressure of 27.7 MPa. If the eastern partial structure Ar1e is modelled separately, an intrusion depth of 0.72 km and a magma pressure of 5.6 MPa is obtained.

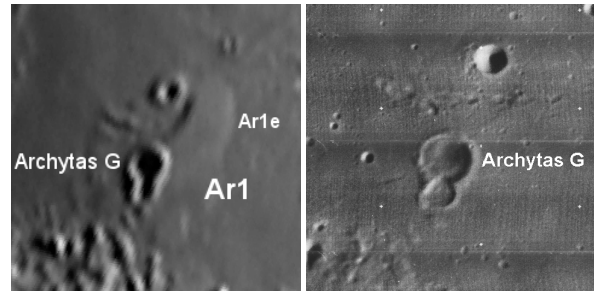


Fig. 1: Left: Telescopic CCD image of the concentric crater Archytas G and the associated intrusive dome Ar1, rectified to perpendicular view. Right: Section of Lunar Orbiter image IV-116-H1.

Spectral analysis. Using Clementine UVVIS imagery, we found that the spectral signature of the floor of Archytas G is similar to that of the highland terrain south of the dome Ar1 (Fig. 2). Especially the 950/750 spectral ratio is similarly high for the concentric crater and the highland soil, where it amounts to about 1.03, indicating a very weak mafic absorption. With its lower 950/750 value of about 1.00, the nearby mare surface is more mafic than the crater floor. An explanation for the relatively high albedo of the mare surface is the mechanism of lateral mixing due to random impacts [7]. The UVVIS spectra show that the impact penetrated the uppermost basaltic layer and indicate at the same time that the shallow crater depth is not due to

lava filling but that the original crater floor is still visible.

Formation of Archytas G: It is suggested in [2] that the modifications of crater morphology which lead to the observed concentric shapes were of volcanic origin. An alternative hypothesis is the formation of concentric craters by impact on a surface consisting of two horizontal layers of different strength [8,9]. According to the analysis of terrestrial concentric craters in [9], the upper layer may e. g. consist of low-strength sedimentary and the lower layer of high-strength crystalline material. The thickness of the upper layer and the position of the interface between the two layers relative to the geometry of the excavation flow are found to be essential factors for the final appearance of the crater. The observation that the large majority of impact craters near the borders of mare regions have normal appearances implies that the presence of a basaltic lava layer of 0.24 km thickness superimposed on the original impact basin floor, as inferred for the dome Ar1, cannot be the reason for the formation of a concentric crater. Moreover, the modelled intrusion depth of Ar1 of 3.5 km is much larger than the inferred depth of the transient cavity of 1.36 km, such that the transient cavity did not reach the intrusive magma body, given the modelling results for Ar1. At the bottom of the transient cavity, however, the flexural rigidity of the overburden and the overburden weight per unit area were reduced to 30% and 61% of their original values, respectively, according to the relations given in [4,10]. If the impact occurred during the magma intrusion phase, the thinned part of the overburden was probably unable to resist the pressurised magma, which in turn may have lifted up the crater floor, thus leading to the shallow crater depth. In this line of thought, the inner depression of the concentric crater is a remnant of the original bowl-shaped crater floor.

On the other hand, if we assume that the intrusive dome Ar1 is made up of two parts and that the intrusion depth corresponds to only 0.74 km as modelled for the eastern partial structure Ar1e, the transient cavity of the impact was about twice as deep as the laccolith overburden. The flexure during laccolith growth may have altered the strength of the crustal material in the overburden by microfracturing [11], resulting in two crustal layers of different strength separated by the comparably thin intrusive magmatic body. The relation between the depth of the transient cavity and the overburden thickness is typical of the types IV and V of the scheme developed in [9] for terrestrial concentric craters. Craters of these types have a rather steep outer rim surrounding a shallow inner depression, formed by uplift, shatter, and subsequent collapse of the upper layer.

Although the similarity of terrestrial type IV and V craters to the concentric crater Archytas G is striking, it should be kept in mind that most type IV and V craters regarded in [9] have diameters well above the simple-to-complex transition, which occurs at a diameter of about 2 km for terrestrial impact craters. Hence, it is questionable if uplift and collapse mechanisms analogous to those identified in [9] have occurred for the concentric crater Archytas G with a diameter well below the lunar simple-to-complex transition limit of about 10 km [12]. On the other hand, an important argument in favour of an origin of lunar concentric craters related to (intrusive) volcanism is the observation that, similar to lunar intrusive domes, the majority of the known concentric craters are located near the borders of mare regions [2]. Hence, many of them may be associated with intrusive magmatic bodies, which do not necessarily all have pronounced surface manifestations.

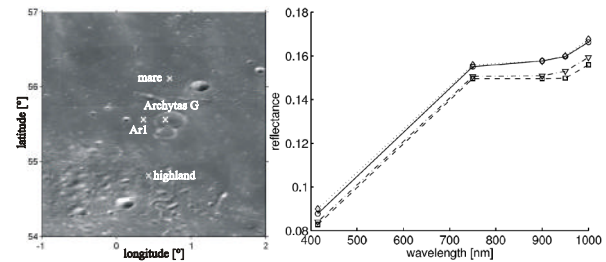


Fig. 2: Left: Clementine 750 nm image of Archytas G and Ar1. Right: Clementine UVIS spectra. Solid curve, circles: Archytas G; dashed curve, squares: Ar1; dashed-dotted curve, triangles: mare surface; dotted curve, diamonds: highland surface.

Conclusion: We have examined the concentric crater Archytas G associated with the intrusive dome Ar1 and have discussed two alternative possible modes of formation: (i) Uplift of the crater floor by the pressurised intrusive magmatic body due to the reduced flexural rigidity of the overburden at the location of the crater; (ii) formation of a concentric crater due to impact on a layered target, followed by layer-specific collapse processes leading to concentric crater morphology. We found several arguments in favour of a formation related to intrusive volcanism, but based on the available observational data and modelling results it is not possible to finally decide which of the two proposed scenarios is the more realistic one.

References: [1] Bugaevskii (1973), *Soviet Astronomy* 16(4); [2] Wood (1978), *LPSC IX*; [3] Wöhler and Lena (2008), *submitted to Icarus*; [4] Kerr and Pollard (1998), *J. Struct. Geol.* 20(12); [5] Wood and Andersson (1978), *LPSC IX*; [6] Lena and Wöhler (2008), *LPSC XXXIX*; [7] Li and Mustard (2000), *J. Geophys. Res.* 105(E8); [8] Piekutowski (1977), *Symp. Planetary Cratering Mechanics*; [9] Abels (2004), *LPSC XXXV*; [10] Jackson and Pollard (1973), *Tectonophysics* 18; [11] Hacker et al. (2007), *Utah Geol. Assoc. Publ.* 35; [12] Pike (1980), *LPSC XI*.